



Mineralogical Study of Borehole MW-206 Asarco Smelter Site Tacoma, Washington





United States Environmental Protection Agency
Region 10, 1200 Sixth Avenue, Seattle, WA 98101-1128

**Mineralogical Study of Borehole MW-206
Asarco Smelter Site
Tacoma, Washington**

October 1, 1998

Prepared by
U.S. Environmental Protection Agency (EPA)
Office of Environmental Assessment
Region 10

CONTRIBUTORS TO STUDY

Project Planning

Office of Environmental Assessment
Workgroup Four, Asarco Sediments/Ground Water Task Force

Field Sampling

John Mefford, Hydrometrics, Inc.

Laboratory Analysis

Sample Preparation and Hydride Generation/Atomic Absorption Analysis
Woodie Campbell, Lockheed Martin, Inc.
USEPA Manchester Laboratory

X-ray Diffraction

David Frank, Office of Environmental Assessment
USEPA Manchester Laboratory

Scanning Electron Microscopy/Electron Microprobe Microanalysis

Bart Cannon, Cannon Microprobe

Report Compilation

David Frank, Office of Environmental Assessment

Site Manager

Lee Marshall, Office of Environmental Cleanup

Study Project Officer

Bernie Zavala, Office of Environmental Assessment

ACKNOWLEDGMENTS

Appreciation for their reviews is extended to Ray Lasmanis and David Norman, Washington State Department of Natural Resources, Division of Geology and Earth Resources; to members of the Asarco Sediments/Ground Water Task Force including Doug Holsten, CH2M Hill, and Scott Mason, Hydrometrics, Inc.; and to Douglas Kendall and Steve Macheimer, USEPA.

DISCLAIMER

Mention of commercial products or trade names is for method documentation and does not constitute endorsement.

CONTENTS

Contributors to Study	ii
Acknowledgments	iii
Disclaimer	iii
Contents	iv
Abstract	1
Introduction	2
Previous Work	2
Methods and Materials	3
Study Design	3
Field Work	3
Laboratory Methods	4
Results	5
Distribution of Minerals	5
Distribution of Arsenic	8
Textural Characteristics of Secondary Minerals	8
Discussion	9
Significance of Secondary Minerals	9
Comparison with Previous Work	10
Conclusions	10
References	11

FIGURES

1. Index map of the Asarco smelter site	15
2. Photograph of slag fragments from 11.5 ft bgs	16
3. Photograph of borehole material from 12.5 ft bgs, showing oxidized coatings	16
4. Graph showing distribution of samples with respect to depth and materials	17
5. Photograph of borehole samples MW-206-1 through MW-206-6	18
6. Photograph of 2-20 mm size fractions of four borehole samples	18
7. BSE image and XRD patterns for ferrihydrite coatings on slag	19
8. BSE image and XRD pattern for symplectite in a coating on slag	20
9. BSE image and XRD pattern for alarsite in a fragment of silica sinter	21
10. Graph showing comparison of arsenic concentrations from bulk analysis and microanalysis	22
11. BSE images of different substrate textures for coatings on slag	23

TABLES

1. Field sample and corresponding laboratory sample numbers	25
2. Field description for boring MW-206	26
3. Summary list of secondary minerals	27
4. Distribution of size separates and corresponding arsenic concentrations	29
5. List of arsenic concentrations from bulk analysis and microanalysis	30

APPENDICES

A. Laboratory Report for Hydride Generation/Atomic Absorption Arsenic Analysis ..	6 pages
B. Laboratory Report for X-ray Diffraction Analysis	58 pages
C. Laboratory Report for Scanning Electron Microscope/Probe Microanalysis	146 pages

ABSTRACT

The mobility of metals in ground water is an important consideration for evaluating remedial options at the Asarco smelter site, Tacoma, Washington. One factor in assessing metal mobility is the degree of secondary mineralization in a slag-fill aquifer extending into the intertidal zone along the Puget Sound shoreline. Samples of aquifer material were collected for mineralogical analysis from borehole MW-206 at five-foot intervals within the slag fill from 5 to 25 feet below the ground surface, and in the underlying marine sand and gravel at 27 feet. Grab samples of slag fragments with visually apparent secondary minerals were also collected at five intermediate depths between 12 and 19 feet. Samples were analyzed by a variety of techniques including hydride generation/atomic absorption for arsenic concentration, scanning electron microscopy/electron microprobe for mineralogical texture and microanalysis, powder x-ray diffraction for mineral identification, and optical microscopy for textural observations.

Siliceous iron oxide hydroxides were found as secondary coatings on the surfaces of slag fragments from borehole MW-206. These precipitation products are most abundant below the water table at depths of 12-20 feet where poorly crystallized ferrihydrite (hydrated iron oxide hydroxide) was identified by x-ray diffraction as the dominant mineral in the coatings. Electron probe microanalysis shows that the coatings are elevated in arsenic content relative to underlying slag, indicating that arsenic from ground water is preferentially incorporated into the coatings. Additional isolated occurrences of secondary copper, iron, lead, zinc, and arsenic-bearing sulfates and hydroxides, lead oxide, and lead carbonate were found by electron microprobe in coatings, pore fillings, and altered sulfides at 12-20 feet. Among these phases, brochantite (copper sulfate hydroxide) was abundant enough to be identified by x-ray diffraction in the ferrihydrite coatings just below the water table at 12.5 feet.

At deeper levels in the borehole near the bottom of the slag fill at 25 feet and in the underlying marine sand and gravel at 27 feet, a variety of metal arsenates were found by microprobe as coatings and void fillings. Among the arsenates, alarsite (anhydrous aluminum arsenate), symplectite and parasymplectite (hydrated iron arsenate), and metakottigite (hydrated iron zinc arsenate) were identified by x-ray diffraction. Alarsite occurred as void-fillings in silica sinter and is believed to be a high-temperature vapor-phase precipitate formed in oven brick. Symplectite and the other iron and zinc arsenates occurred in coatings on slag surfaces and are believed to be low-temperature precipitation products from ground water. The distribution of arsenic as measured by both bulk chemical analysis and electron probe microanalysis suggest that the alarsite is a major arsenic-bearing phase in the lower part of the borehole.

The distribution and texture of secondary minerals indicate that mineral precipitation from ground water should be contributing to a decrease in arsenic concentration in the upper part of the slag fill at borehole MW-206 where arsenic-bearing ferrihydrite coatings are abundant. In contrast, the metal arsenates at the bottom of the slag fill and in the marine sand and gravel do not provide supporting evidence for decreasing arsenic concentrations in ground water by secondary mineralization. Mineralogical limitations include the occurrence of alarsite which cannot be attributed to precipitation from ground water and the symplectite and other hydrated iron and zinc arsenates which, along with alarsite, have uncertain long-term stability at neutral or alkaline ground water conditions.

INTRODUCTION

Remedial planning for the Asarco smelter site in Tacoma, Washington, requires an understanding of the geochemical processes affecting the fate of contaminants in ground water. Smelter slag was used as fill in the intertidal zone along the Puget Sound shoreline. The slag fill and underlying marine sand and gravel are now traversed by contaminated ground water. A remedial question of concern is whether metals transported by ground water from source areas are precipitating onto slag surfaces as secondary minerals, resulting in a decrease in downgradient concentrations in ground water. The objective of this study is to identify metal-bearing phases in the slag-fill aquifer, with an emphasis on the characteristics of secondary minerals especially those containing arsenic. The goal is to aid in understanding geochemical controls on metal mobility in ground water under current or changing environmental conditions.

Some of the terms used here may warrant clarification. “Metals”, as used in this report, also refers to metalloids such as arsenic. “Minerals”, by strict definition, refers to naturally occurring compounds. Although man-made slag compounds are not natural minerals, they are described here by their mineral analog in cases where compound identification can be analytically matched to a unique mineral composition and structure. “Phase” is used here in the general sense for a particular composition of mineral or other compound regardless if naturally occurring or man-made. Primary minerals or phases are those believed to be an original part of the solid matrix. Secondary minerals or phases are those believed to have formed as coatings or void fillings after formation of the solid matrix, or as in-situ alteration products of primary phases.

PREVIOUS WORK

Lasmanis and others (1997) used scanning electron microscopy/electron microprobe analysis, and x-ray diffraction to identify a large variety of slag compounds and secondary minerals from the Asarco smelter site. They describe the slag as a volcanic rock-like material with a variety of silicates and metal oxides, arsenides, antimonides, selenides, telluride, sulfides, and alloys. Secondary minerals identified in their study include metal arsenates, chlorides and chlorates, hydroxides, phosphates, and sulfates. The results of Lasmanis and others (1997) provide a record of mineral alteration and precipitation at the marine interface. Their samples were collected in the intertidal zone from the surface of the slag fill. As such, the results of Lasmanis and others (1997) should represent an environment where the metal concentrations in ground water seepage would be diluted by seawater mixing and where oxidation would be enhanced by repetitive open-air wetting and drying during the tidal cycle.

The intent of the current study is to acquire similar mineralogical information from upgradient in the ground water system, where seawater dilution and atmospheric exposure would be less than at the shoreline.

METHODS AND MATERIALS

Study Design

Drill cuttings were collected from the slag fill and underlying marine sand and gravel in a borehole located between a source of arsenic waste (the arsenic kitchens) and the Puget Sound shoreline. The cuttings were analyzed for arsenic concentration by hydride generation/atomic absorption, and for mineralogy by scanning electron microscopy/electron microprobe, x-ray diffraction, and low-power optical microscopy. A sample preparation procedure was used to separate grain sizes as a means of concentrating mineral phases associated with particular size ranges. The crushing and grinding action of the drilling procedure was expected to preferentially reduce the size of softer secondary minerals. Accordingly, a fine-grained separate was prepared to provide a concentrate of secondary minerals. The coarser-grained separates, on the other hand, provided larger-sized material expected to have intact coatings made up of relatively harder secondary minerals.

Field Work

Cuttings samples were collected from a ten-inch borehole (MW-206) during November 18-20, 1997, by Hydrometrics, Inc. The borehole was sited for installation of a six-inch well to be used for a pump test of the slag aquifer. The borehole was also suitable for the mineralogical study by being located approximately in the middle of the slag fill in an area known to be traversed by ground water with elevated arsenic concentrations. The location was 250 feet (ft) from the Puget Sound shoreline, northeast of the fine-ore storage building (Figure 1).

The borehole was drilled with a Model 71 Speedstar cable tool rig. Samples were extracted from the hole with a six-inch sand pump (Figure 2), and collected in 1-quart glass jars. The collection procedure included all size fractions from fines to cobbles. Because of the use of a cable tool and large sand pump, several cobble-sized fragments greater than 20 mm across were obtained. Samples MW-206-1 through MW-206-5 were collected at five-foot intervals within the slag fill from 5 to 25 ft below the ground surface (bgs) (Table 1). Sample MW-206-6 was collected from the underlying marine sand and gravel at 27 ft bgs. These six samples are representative of the full size range of material available from the sand pump. Grab samples of cobble-size slag fragments with observable mineral coatings were also collected at five intermediate depths between 12 and 19 ft (Figure 3), placed in a sample jar in individual bags marked for each depth and labeled as a composite sample. After obtaining the last sample at 27 ft bgs, custody of all samples was transferred from Hydrometrics to EPA on November 20 and transported to the Manchester Laboratory.

Table 2 contains information from the Test Log Field Form prepared by John Mefford, Hydrometrics, on the geologic description and drilling characteristics for the borehole. The borehole log indicates that the water table occurred at a depth of about 8-9 ft, and that the slag varies between areas of massive slag with little void space to less indurated slag with many

voids. Figure 4 provides a diagram of sample location relative to depth and lithologic materials. The drilling time shown in Figure 4, as estimated from sample times and field notes, indicates variations in induration of the slag unit with higher rates occurring in less massive sections having greater void space.

Laboratory Methods

Approximately 500 g each of samples MW-206-1 through MW-206-6 were separated by wet sieving to produce five size fractions: <0.07 mm (silt), 0.07-0.5 mm (fine sand), 0.5-2 mm (coarse sand), 2-20 mm (gravel), and >20 mm (cobble). Sample MW-206-7, which was the composite of cobble-size fragments from intermediate depths, was separated into five laboratory samples specific to the original respective depths. Each separate was assigned a new lab number for a total of 27 laboratory samples generated from the original seven field samples.

Following size separation, samples were split for analysis by different analytical procedures. Splits of the silt fractions (<0.07 mm) and the combined fine and coarse sand fractions (0.07-2 mm) were sent for hydride generation/atomic absorption analysis at the Manchester Laboratory. Splits of all size fractions were provided to both the x-ray diffraction (XRD) facility at the Manchester Laboratory and to Cannon Microprobe, Seattle. All cobble-size fragments (>20 mm) were split with a diamond saw and provided to both the XRD and microprobe facilities.

Arsenic analysis was performed at the Manchester Laboratory using hydride generation/atomic absorption spectroscopy with a Perkin Elmer 3110 spectrophotometer (USEPA SW 846 Method 7061A). A detection limit of 10 mg/kg was achieved by the method. The laboratory report for arsenic analysis is in Appendix A.

X-ray diffraction analysis was accomplished at the Manchester Laboratory with a Scintag X1 powder diffractometer using CuK α radiation at 40 ma and 45 kv. Diffractograms were recorded at scan speeds of 15 degrees and 0.5 degrees of two-theta units per minute over a 2-64 degree range. The method provided qualitative identification of minerals greater than a few percent in concentration. Identifications were made by matching measured diffraction patterns with a database maintained by the International Centre for Diffraction Data (ICDD) and with measured reference samples. A Frantz magnetic barrier separator was used for magnetic separations of some samples to provide mineral concentrates for XRD analysis. Microscopic observations at low power using a binocular scope with incident light were also made in conjunction with the XRD analysis. The XRD laboratory report is in Appendix B and contains a summary list of detected phases, peak lists for measured diffraction patterns and comparative ICDD database patterns, annotated diffractograms, sample preparation information, and notes on microscopic observations.

Scanning electron microscopy/electron microprobe analysis (SEM/EPMA) was performed at Cannon Microprobe, Seattle, using an ARL SEMQ electron microprobe at 25 kv

and 50 na beam current. Both grain mounts and polished sections were prepared as specimens. Scanning electron microscope images were made in the backscattered electron detection mode (BSE images) by which image contrast is a function of atomic number. Microanalysis was accomplished with the probe using a Kevex energy-dispersive x-ray spectrometer (EDS) for rapid detection of several elements, and six wavelength-dispersive x-ray spectrometers (WDS) for quantitation of iron, arsenic, oxygen, lead, zinc, and copper. The microprobe report is in Appendix C and is arranged with data presented in four parts for each sample, including a narrative discussion of the distribution of arsenic, a group of BSE images, a list of WDS analyses for six elements, and a group of EDS spectra.

RESULTS

All samples in bulk appeared generally as dark gray fragmental material (Figure 5). Reddish brown coatings were present on many of the larger clasts for all samples, and scattered light-colored fragments occurred in the lowest two samples from 25-27 ft bgs. Figure 6 shows the 2-20 mm fraction of samples MW-206-4 through MW-206-6 from 15-27 ft bgs. Light-colored fragments noted as cinderstone in the borehole log (Table 2) are apparent in the 25-ft slag sample. Light-colored rocks and shells making up beach gravel are apparent in the 27-ft marine sample.

Distribution of Minerals

The samples from the slag unit (MW-206-1 through MW-206-5, and MW-206-7) consist largely of iron-rich silicate phases and metal oxides in a black, dark brown, or dark gray indurated matrix that ranges from fine-grained to porphyritic in texture (Appendices B and C). The two most abundant primary silicate phases are analogous to the olivine mineral (fayalite) and a pyroxene mineral (ferroaugite). The most abundant metal oxides are magnetite and maghemite. Several lesser abundant primary phases are noted in the microprobe and XRD reports, including other silicates, silicate glass, sulfides and arsenides. In particular, clusters of sulfides occur as immiscible droplets in the slag matrix. When occurring as shot-sized inclusions or granules, the sulfides are referred to as prills in the microprobe report. Solid solution appears to be common in the slag, whereby trace to minor amounts of arsenic, copper and other metals can be detected by microprobe in most phases. The results in this study for the primary slag phases are consistent with work by Dabbs (1984) on fayalite slag and with the shoreline mineralogy study by Lasmanis and others (1997).

Several secondary minerals were identified as precipitation products on slag surfaces and as alteration products of primary slag phases, and are discussed below. Other materials found in the slag unit, besides slag, include sparse siliceous inclusions of quartz and feldspar, and sparse wood fragments. The quartz/feldspar inclusions appear to have originated in the flux used in the smelting process. In addition, the lowermost slag sample at 25 ft bgs (MW-206-5) contains abundant fragments of silica sinter, noted as cinderstone in the borehole log (Table 2) and as ceramic in the XRD report (Appendix B). The sinter is composed mainly of quartz (SiO₂) and

cristobalite (also SiO_2) with lesser corundum (Al_2O_3), and would be consistent with an origin in oven brick. The silica sinter contains a large component of aluminum arsenate as discussed below.

The sample of the marine sand and gravel at 27 ft bgs (MW-206-6) consists mostly of common rock-forming minerals found in typical Puget Sound beach deposits, including quartz, feldspar, mica, chlorite, amphibole, aragonite (in clam shells), and other lesser abundant minerals. In addition, the marine sample also contains slag and silica sinter similar to that found in the overlying sample of the slag unit.

Table 3 provides a summary list of secondary minerals identified in the microprobe and XRD reports (Appendices B and C). The table is arranged by increasing depth of sample. Qualitative terms used in the table are taken from the laboratory reports. For the XRD identifications, major indicates approximately greater than 20% abundance, minor is about 3-20%, and trace is generally less than 3%.

The most visually prominent secondary mineralization is reddish brown to brown coatings on slag surfaces in samples from below the water table (see Figures 2-3). The microprobe report notes that the coatings are either somewhat common or common in samples from 12-27 ft bgs, and absent or not observed in shallower samples at 5 and 10 ft (Table 3). The microprobe report describes the coatings as an iron hydroxide or iron silicon hydroxide. The XRD report identifies the predominant phase in the coatings on samples between 12-20 ft as ferrihydrite. Figure 7 shows corresponding microprobe and XRD data for coatings on slag fragments from sample MW 206-7. The scanning electron microscope BSE image is of a polished section that shows a spongy, fine-grained coating (Si and As bearing FeHOX , Figure 7) covering the larger-grained silicate slag matrix (fayalite). The XRD pattern of coating material scraped off the slag fragments shows a poorly crystallized variety of ferrihydrite termed two-line ferrihydrite for two broad diffraction peaks.

Ferrihydrite is a poorly crystallized, very fine-grained secondary iron mineral that has been described as having a stoichiometry of FeOOH , "...modified by small crystal size and high surface water content to a composition of between $\text{Fe}_4(\text{OH})_{12}$ and $\text{Fe}_5\text{O}_3(\text{OH})_9$ " (Eggleton and Fitzpatrick, 1988, p. 123). Many variations may be found in the literature for the formula of ferrihydrite. That used here ($\text{Fe}_5\text{O}_7\text{OH}\cdot 4\text{H}_2\text{O}$) is from the XRD database and agrees with the most commonly reported proportion of elements, $\text{Fe}_5\text{O}_{12}\text{H}_9$. The microprobe report notes that most microanalyses of the coatings show appreciable silicon content. Studies of ferrihydrite indicate silicon can be a common constituent of up to 9% (Parfitt and others, 1992). The phase believed to be dominant in the slag coatings is siliceous ferrihydrite. Goethite (FeOOH), a mineral that has been considered an aging product of ferrihydrite, was also identified by XRD in trace amounts both in the ferrihydrite coatings and in the silt-sized separates.

Other less abundant secondary minerals were identified as components mixed with the ferrihydrite coating or as separate coatings (Table 3). The most prominent include brochantite

($\text{Cu}_4\text{SO}_4(\text{OH})_6$), identified by XRD in a ferrihydrite coating from 12.5 ft bgs (Figure 7), and a variety of arsenates dominated by symplectite ($\text{Fe}_3(\text{AsO}_4)_2 \cdot 8\text{H}_2\text{O}$) in a coating at 25 ft bgs. Other similar arsenates identified by XRD in the coating at 25 ft bgs include parasymplectite ($\text{Fe}_3(\text{AsO}_4)_2 \cdot 8\text{H}_2\text{O}$) and metakottigite [$(\text{Fe,Zn})_3(\text{AsO}_4)_2 \cdot 8(\text{H}_2\text{O,OH})$]. Corresponding microprobe data that is consistent with these minerals include copper iron sulfates in coatings at 12-19 ft and several metal arsenates occurring both in coatings and as pore fillings at 25 ft (Table 3). Figure 8 shows corresponding microprobe and XRD data for symplectite. The BSE image in Figure 8 is of a grain mount showing coarse-grained, radiating plates of symplectite crystals emerging from a coating on a slag fragment. The XRD pattern of coating scraped off a split of the same slag fragment shows prominent diffraction peaks for well crystallized symplectite and metakottigite.

The most abundant arsenic-bearing mineral found at 25-ft bgs (MW-206-5) in borehole MW-206 is alarsite (AlAsO_4) and occurs as pore fillings in the silica sinter. The alarsite was identified both by XRD and microprobe. Although alarsite is probably a smelter waste product, it is discussed here with secondary minerals because of its mode of occurrence as a pore filling, similar to other secondary minerals. Alarsite is the mineral name for aluminum arsenate, more commonly known as an experimental laboratory compound. The natural mineral is found as a high temperature vapor-phase precipitate near volcanic fumaroles (Semenova and others, 1996). Alarsite would not be expected to be a primary phase in either slag or sinter. The similarity of the silica sinter to oven material suggests that the alarsite formed as a secondary vapor-phase precipitate in oven brick. The same phase is also found in the silt fraction of MW-206-5. Figure 9 shows corresponding microprobe and XRD data for alarsite. The BSE image is of a polished section of a sinter fragment embedded in mounting epoxy. Fine-grained alarsite (brighter grains in Figure 9) is scattered in the pore spaces among coarser grained silica. The XRD pattern for silica sinter fragments from a split of the same sample shows prominent diffraction peaks for well crystallized alarsite along with quartz and cristobalite which make up the silica matrix (Figure 9).

Secondary minerals in sample MW-206-6 of the marine unit at 27 ft bgs are similar, though less abundant, to those in the immediately overlying slag sample from 25 ft (Table 3). The potential mixing of slag and silica sinter with the upper part of the marine sand and gravel during slag emplacement suggests a probable source for minerals such as iron oxide hydroxides and alarsite found in the marine unit. Alternatively, the iron oxide hydroxide coatings may have also formed in the marine unit as a result of precipitation from ground water.

Isolated amounts of other secondary minerals were identified by microprobe as possible alteration products of sulfides and arsenides at several depths (Table 3). These include copper, zinc, lead, and arsenic bearing sulfates, hydroxides, carbonates and arsenates. The presence of sulfides was noted in the microprobe analysis to be relatively sparse, consisting of a fraction of a percent of the separates for all samples. Furthermore, review of BSE images in Appendix C indicates that relict sulfide shapes or grains that would provide clear evidence of sulfide alteration are uncommon. Therefore the sulfide alteration products are also believed to be less abundant than precipitated coatings.

Distribution of Arsenic

For the silt fractions of slag samples, arsenic concentrations generally increase with the depth of sample, ranging from 140 mg/kg in the silt fraction of the 5-foot sample to over 1% in the 20-25 foot samples (Table 4 and Appendix A). The sample of the underlying marine unit has an arsenic concentration in the silt fraction almost as high as that in the overlying slag (9360 mg/kg in the marine unit and 10,900 mg/kg in slag). The increase in arsenic concentration with depth in the bulk silt fraction corresponds to an increase in the microprobe-analyzed content of the fine fraction and to the occurrence of arsenate minerals in coatings and silica sinter.

Figure 10 shows the relationship between arsenic concentration from both bulk and microanalysis of the silt fractions (fines), and microanalysis of three other material types grouped as silicates, sulfides, and coatings. The probe values plotted in Figure 10 are calculated as geometric means (Table 5) of values taken from the WDS tables of data for six elements as listed in the microprobe report (Appendix C). Prior to calculation of the geometric means, the Appendix C tables were first edited to eliminate analyses that were either labeled questionable (??), or noted by reference to BSE images to be part of an alternative materials group.

Figure 10 indicates that the arsenic content of both coatings and fines is greater than that of the silicate matrix of all samples. Furthermore, the arsenic content of either the coatings or the fines, or both, are generally greater than that of the sulfides. Considering that the coatings are secondary minerals and that the fines are a concentrate of secondary minerals, Figure 10 suggests that the secondary minerals have concentrated arsenic relative to the primary slag phases.

Textural Characteristics of Secondary Minerals

Textural relationships evident in the BSE images (Figure 11 and Appendix C) indicate that much of the iron oxide hydroxide coatings are precipitates from ground water. For example, image #4@528 in Figure 11 is of a polished section that shows an iron silicon hydroxide coating caked onto the smooth surface of underlying fayalite that makes up the matrix of the slag fragment. In other examples, some of the BSE images show coatings on heavily pitted slag surfaces, such as the polished section in BSE image #7Xh2 (Figure 11), suggesting in-place alteration of the slag matrix. The predominance of one mode of coating formation (precipitation from ground water) over another (in-place alteration) is difficult to determine with certainty from available data. The more common occurrence of a precipitation-type of texture, indicated by a smooth interface between coating and underlying slag matrix (see BSE images in Appendix C), suggests that precipitation of iron oxide hydroxide is an active process in most of the slag fill.

Textural evidence indicates that the coarser-grained hydrated iron and zinc arsenate coatings at 25 ft bgs are precipitation products that formed from ground water. Key features include the occurrence as coatings with free crystal surfaces rather than as enclosed or included

grains, and the presence of unbroken euhedral symplectite crystal shapes as seen in BSE images (Figure 8). Evidence that the arsenate crystals are relatively fresh rather than relicts of formation during hot slag dumping are their lack of obvious alteration features on the surfaces of coarse-grained symplectite. However, formation in seawater also as slag cooled is not necessarily precluded for any of the secondary minerals, including ferrihydrite.

DISCUSSION

Significance of Secondary Minerals

The suite of secondary minerals found in borehole MW-206 provides information on the environmental conditions under which the minerals formed, and on their stability should those conditions change.

Ferrihydrite forms under oxidizing conditions as a metastable mineral that should alter with time to either goethite or hematite, with goethite favored at a lower pH of 4-6 and hematite at a pH of 7-8 (Schwertmann and Taylor, 1989). The identification of trace amounts of goethite and the siliceous characteristics of the FeSi hydroxide in probe analyses indicate that siliceous ferrihydrite is forming under somewhat acidic but oxidizing conditions. The bright reddish brown color of coatings just below the water table are consistent with ferrihydrite forming in perhaps the most oxidized part of the borehole section, close to the water table. The XRD data suggest that ferrihydrite decreases with depth in that it is not abundant enough to be detected below 20 ft, although the microprobe results provide evidence of continued occurrence of FeSi hydroxide to the bottom of the borehole.

The occurrence of brochantite is also an indication of oxidizing conditions, as well as elevated sulfate (Woods and Garrels (1986). Brochantite was only identified just below the water table at 12.5 ft, and would suggest that conditions for its formation may not occur deeper in the borehole.

Evaluation of the full significance of the occurrence of the iron, zinc, and aluminum arsenates (symplectite, parasymplectite, metakottigite, alarsite) at the bottom of the slag fill is beyond the scope of this report because of limited information on solubilities. However, some inferences can be made by comparison with similar phases described in the literature. References to stability fields for arsenates with similar composition to those found in the slag fill indicate a range of stability from low pH to slightly alkaline pH; for example, anhydrous ferric iron arsenate - FeAsO_4 (pH < 4, Robins, 1982, p. 298), scorodite - perhaps the most commonly found hydrated ferric iron arsenate - $\text{FeAsO}_4 \cdot 2\text{H}_2\text{O}$ (pH < 4, Dove and Rimstidt, 1985), anhydrous zinc arsenate - $\text{Zn}_3(\text{AsO}_4)_2$ (pH 3-8, Robins, 1982, p. 296), kottigite - the zinc end-member of the kottigite-metakottigite-symplectite series - $\text{Zn}_3(\text{AsO}_4)_2 \cdot 8\text{H}_2\text{O}$ (pH < 4, Magalhaes and others, 1988, p. 685), and anhydrous aluminum arsenate - AlAsO_4 (pH 2-7, Robins, 1982, p. 299).

In general, the presence of the particular arsenates found near the base of the slag fill

suggest that stable conditions would require somewhat lower pH and (because of the reduced iron in symplectite) lower oxidation potential than shallower depths having more abundant ferrihydrite. Alternatively, the arsenate minerals may not be in a stable environment. Site-specific solubility calculations would be needed to better estimate the long-term stability of the arsenates. In comparison to ferrihydrite and its aging products, goethite or hematite, the arsenates would appear to have less certain long-term stability under near-neutral or alkaline, oxidizing conditions

Comparison with Previous Work

The results from this study, though not inconsistent with those of Lasmanis and others (1997), differ in two significant respects. First, some of the materials encountered in sampling the slag differed between the two studies. Second, fewer and somewhat different secondary minerals were found in the borehole samples, compared to the previous work on shoreline samples.

With respect to materials, the shoreline study encountered more sulfide-rich material that may have a bearing on the type and amount of secondary minerals. Slag cones and sulfide-rich matte found at the shoreline, for example, were not encountered in the borehole. On the other hand, the borehole samples contained arsenic-bearing silica sinter which was not examined in the shoreline study. Furthermore, the aqueous environment at the shoreline is marine water, whereas the borehole contained more dilute ground water mixed with marine water. The differences in secondary mineralization appear to reflect the differences in materials and environment. Lasmanis and others (1997) reported in detail a variety of metal chloride minerals along the shoreline, with copper chlorides being the most abundant group of secondary minerals. The occurrence of chlorides was not confirmed in the borehole samples. Arsenates, however, were a major part of the secondary mineralization near the bottom of the borehole, but were apparently not abundant at the shoreline.

Though seemingly homogenous at first glance, the heterogeneity of both the slag fill and the local ground water environment would be important controls on secondary mineralization. Therefore a qualification for both the shoreline study and this borehole study is that they are representative only of those areas sampled.

CONCLUSIONS

Siliceous iron oxide hydroxides occur as secondary coatings on surfaces of slag fragments from borehole MW-206. These coatings are products of precipitation from ground water and are most abundant below the water table at 12-20 ft bgs where poorly crystallized ferrihydrite was identified by XRD as the dominant mineral in the coatings. Electron probe microanalysis shows that the coatings are elevated in arsenic content relative to underlying slag, indicating that arsenic from ground water is preferentially incorporated into the coatings.

Copper sulfate hydroxide also occurs in the ferrihydrite coatings just below the water table at 12.5 ft bgs where brochantite was identified by XRD. Other isolated occurrences of secondary copper, iron, lead, zinc, and arsenic-bearing sulfates and hydroxides, lead oxide, and lead carbonate were identified by electron microprobe in coatings, pore fillings, and altered sulfides at 12-20 ft bgs, but were not abundant enough to be identifiable by XRD as discrete minerals.

At deeper levels in the borehole near the bottom of the slag fill at 25 ft bgs and in the underlying marine sand and gravel at 27 ft bgs, a variety of metal arsenates occur as coatings and void fillings. The most abundant of the arsenates, alarsite and symplectite, were identified by both XRD and microprobe in this zone. The distribution of arsenic as measured by both bulk chemical analysis and electron probe microanalysis suggest that the alarsite, occurring as void fillings in silica sinter, is a major arsenic-bearing phase in the lower part of the borehole. The alarsite, an anhydrous aluminum arsenate, is believed to be a high-temperature precipitation product formed from a vapor phase during smelting. The symplectite and other similar hydrated iron and zinc arsenates identified by XRD, parasymplectite and metakottigite, are believed to be precipitation products from ground water.

The distribution and textural characteristics of the secondary minerals indicate that at borehole MW-206 mineral precipitation from ground water should be contributing to a decrease in metals concentration in the upper part of the slag fill where arsenic-bearing ferrihydrite coatings are most abundant. These coatings should remain stable or age to goethite under continued near-neutral oxidizing conditions in the slag fill where shallow ground water mixes with oxidized marine water.

The same conclusion cannot be made for the lower part of the slag fill and the underlying marine sand and gravel because of the occurrence of anhydrous aluminum arsenate which cannot be attributed to precipitation of ground water and because of the hydrated iron and zinc arsenates which, along with aluminum arsenate, may have limited long-term stability at neutral or alkaline ground water conditions.

REFERENCES

- Dabbs, Daniel M., 1984, The physical chemistry of arsenic in fayalite slag: Seattle, University of Washington, Ph.D. dissertation, 219 p.
- Dove, Patricia Martin and Rimstidt, J. Donald, 1985, The solubility and stability of scorodite, $\text{FeAsO}_4 \cdot 2\text{H}_2\text{O}$: *American Mineralogist*, v. 70, p. 838-844.
- Eggleton, Richard A. And Fitzpatrick, Robert W., 1988, New data and a revised structural model for ferrihydrite: *Clays and Clay Minerals*, v. 36, no. 2, p. 111-124.
- Lasmanis, Raymond L., Norman, David K., and Cannon, Bart, 1997, Preliminary study of

- minerals in Tacoma smelter slags: *Washington Geology*, v. 25, no. 3, p. 19-25.
- Magalhaes, M. Clara F., Pedrosa de Jesus, Julio D., and Williams, Peter A., 1988, The chemistry of formation of some secondary arsenate minerals of Cu(II), Zn(II) and Pb(II): *Mineralogical Magazine*, v. 52, p. 679-690.
- Parfitt, R.L., Van der Gaast, S.J., and Childs, C.W., 1992, A new structural model for natural siliceous ferrihydrite: *Clays and Clay Minerals*, v. 40, no. 6, p. 675-681.
- Robins, R.G., 1982, The stabilities of arsenic (V) and arsenic (III) compounds in aqueous metal extraction systems in Osseo-Assare, K. and Miller, J.D., (eds.), *Hydrometallurgy, Research Development and Plant Practice*: Warrendale, Pennsylvania, TMS, The Metallurgical Society, p. 291-310.
- Schwertmann, U. And Taylor, R.M., 1989, Iron oxides in Dixon, J.B. and Weed, S.B. (eds.), *Minerals in soil environments: Soil Science Society of America Book Series no. 1*, p. 379-438.
- Semenova, T.F., Vergasova, L.P., Filatov, S.K., and Ananov, V.V., 1996, Alarsite $AlAsO_4$, a new mineral of volcanic exhalations: *Doklady Akademi Nauk, Earth Science*, v. 342, p. 125-130. (Translated from *Doklady Akademi Nauk*, 1994, v. 338, no. 4, p. 501-505.)
- Woods, Terri L. And Garrels, Robert M., 1987, Use of oxidized copper minerals as environmental indicators: *Applied Geochemistry*, v. 1, p.181-187.

List of Figures

1. Index map of the Asarco smelter site.
2. Photograph of slag fragments from 11.5 bgs removed borehole MW-206 by the sand pump.
3. Photograph of borehole material from 12.5 ft bgs, showing oxidized coatings on fragments.
4. Graph showing distribution of samples with respect to depth and materials.
5. Photograph of borehole samples MW-206-1 through MW-206-6.
6. Photograph of 2-20 mm size fractions of four borehole samples.
7. BSE image and XRD patterns for ferrihydrite coatings on slag.
8. BSE image and XRD pattern for symplectite in a coating on slag.
9. BSE image and XRD pattern for alarsite in a fragment of silica sinter.
10. Graph showing comparison of arsenic concentrations from bulk analysis and microanalysis.
11. BSE images of different substrate textures for coatings on slag.

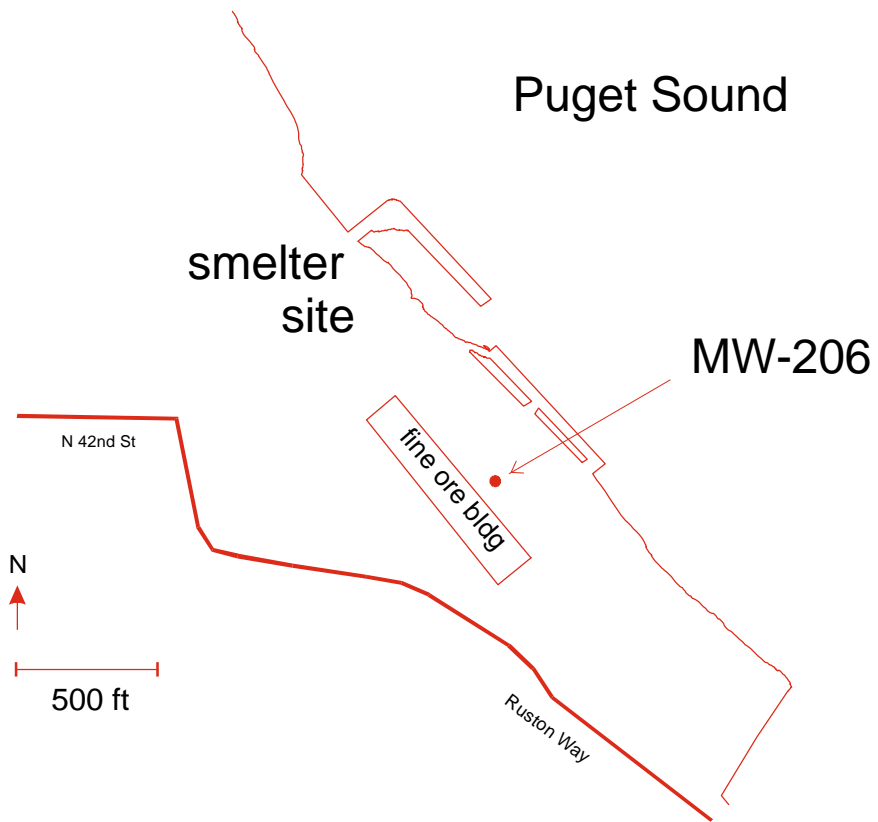


Figure 1. Index map of the Asarco smelter site. Borehole MW-206 is about 300 ft from the Puget Sound shoreline NE of the fine ore storage building.



Figure 2. Slag fragments from 11.5 ft bgs removed from borehole MW-206 by the sand pump, November 19, 1997.

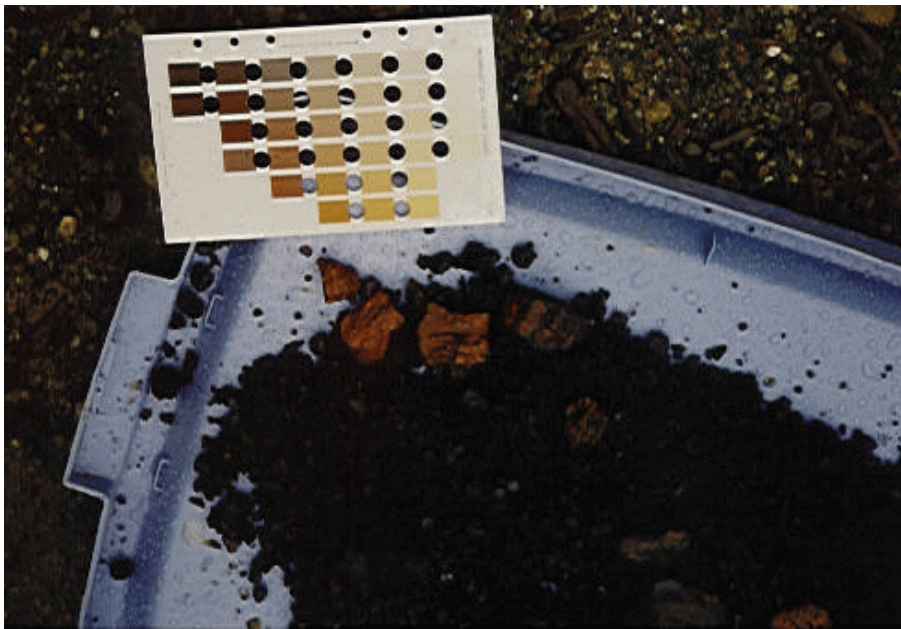


Figure 3. Photograph of borehole material from 12.5 ft bgs, showing oxidized coatings on slag fragments, November 19, 1997. Coating colors match 5YR 6/8 (reddish yellow) and 5YR 5/8 (yellowish red) on the Munsell Soil Color Chart.

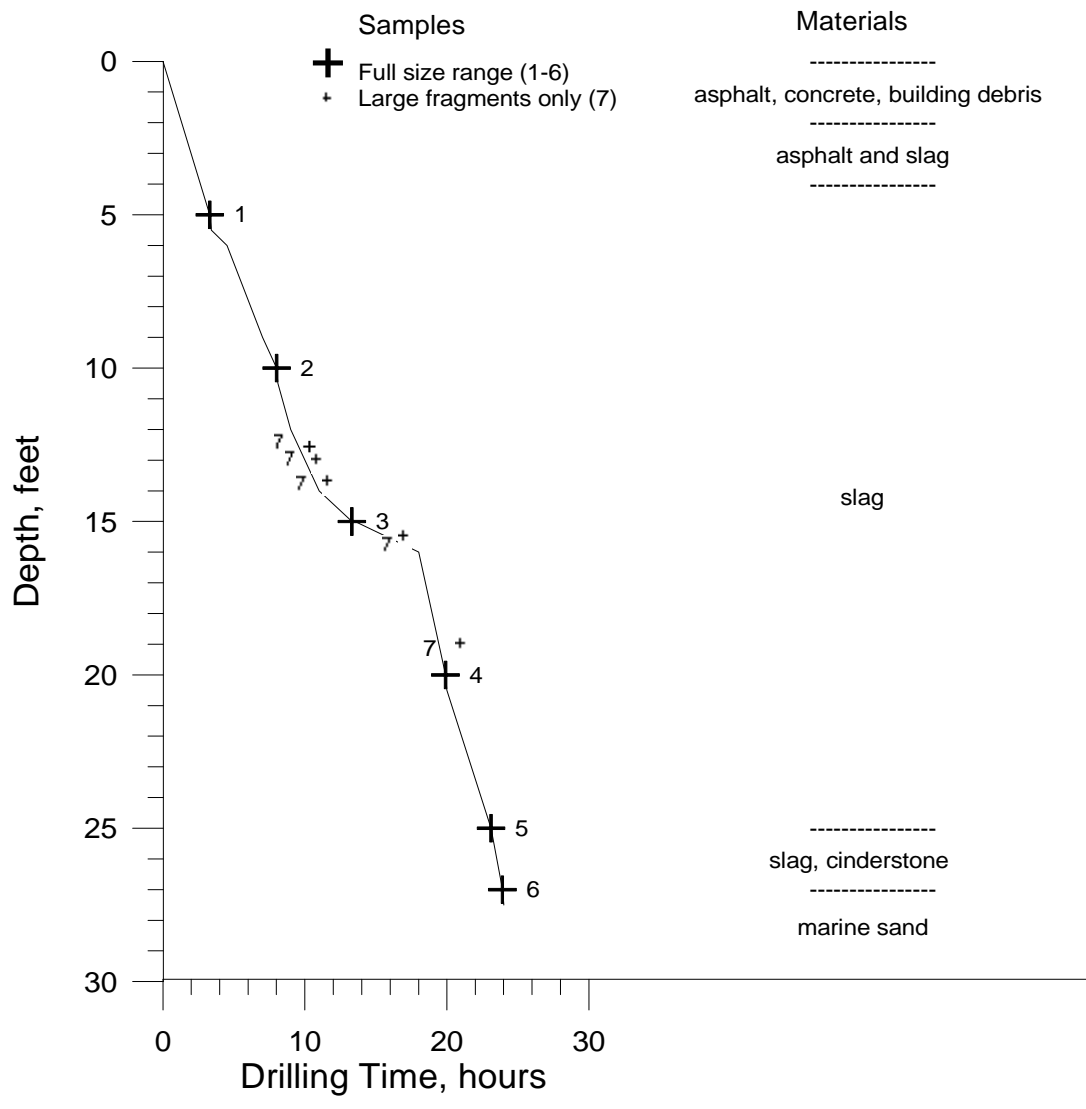


Figure 4. Distribution of samples with respect to depth and materials. The variation in drilling time indicates a massive section of slag occurs at a depth of 14-17 feet. Data are taken from the borehole log prepared by Hydrometrics, Inc.

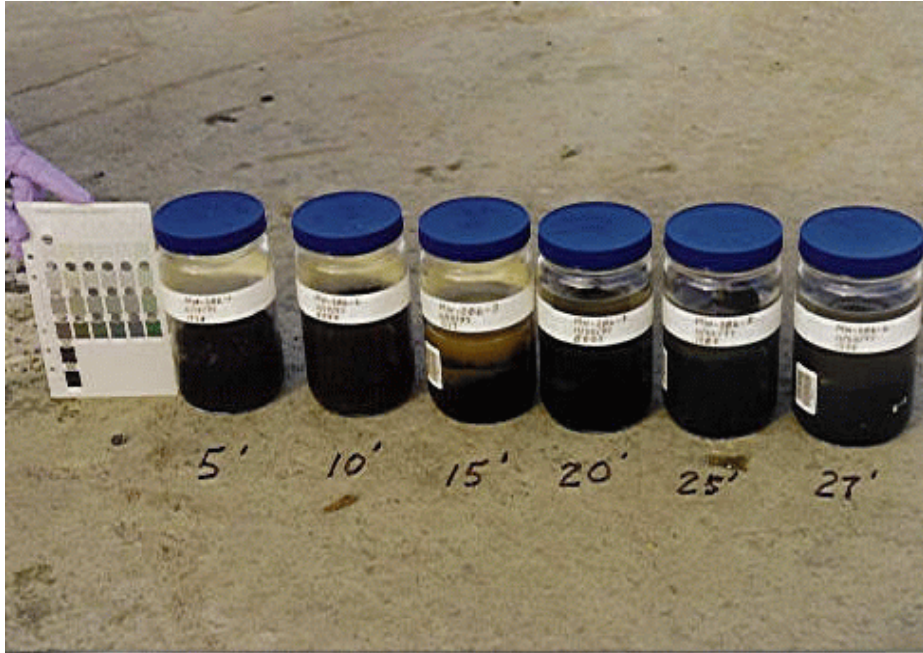


Figure 5. Borehole samples MW-206-1 through MW-206-6 collected November 18-20 from the depths noted. Most of the solids are dark gray. Yellowish brown water in sample MW-206-3 (15 ft) is representative of color discharged from just below the water table. White fragments apparent in sample MW-206-6 are pieces of clam shell.



Figure 6. Coarse size fractions (2-20 mm) of four borehole samples from MW-206 from the depths noted. See text for discussion.

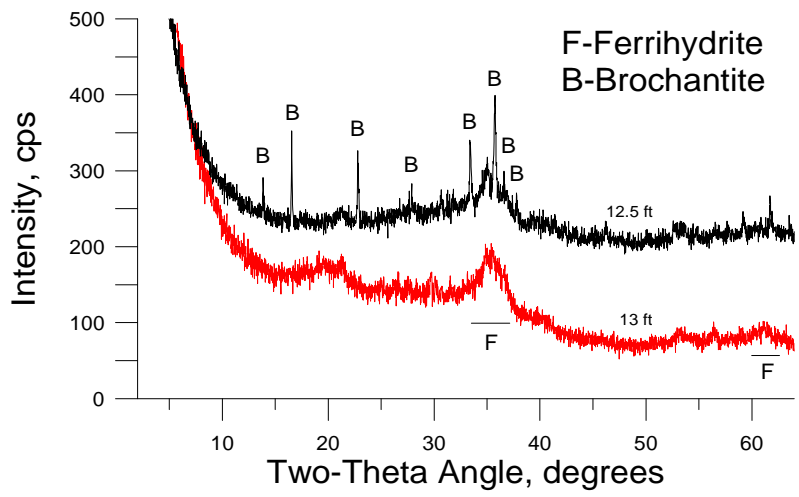
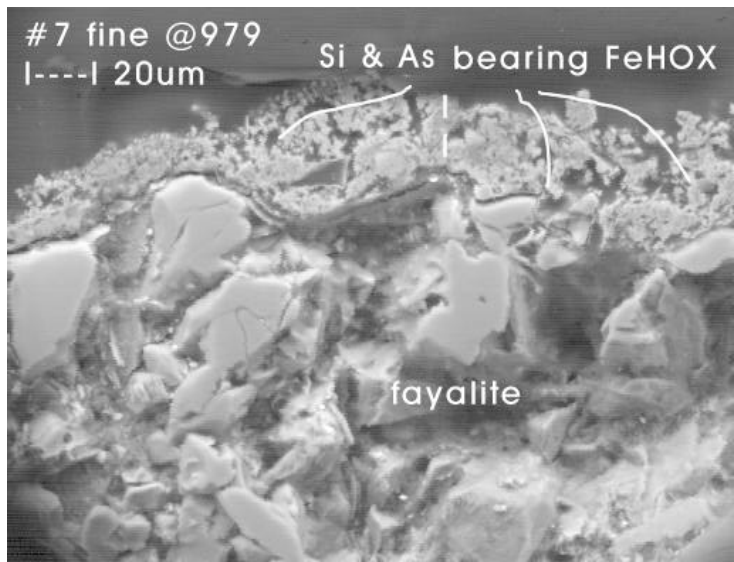


Figure 7. Scanning electron microscope BSE image and corresponding x-ray diffractograms of coatings on fayalite slag fragments from sample MW-206-7. Texture and EDS spectra of similar coatings indicate a composition of siliceous arsenic-bearing iron hydroxides; WDS analysis #979 shows 40% iron and 6820 mg/kg arsenic in the coating. XRD analysis of similar coatings show them to be predominantly 2-line ferrihydrite. Other minerals showing up in XRD patterns of coatings include small peaks for goethite and underlying silicates. The upper pattern shows major peaks for brochantite, which is observable under the microscope as emerald green crystals embedded in coating material on slag from 12.5 feet bgs. BSE image by Cannon Microprobe.

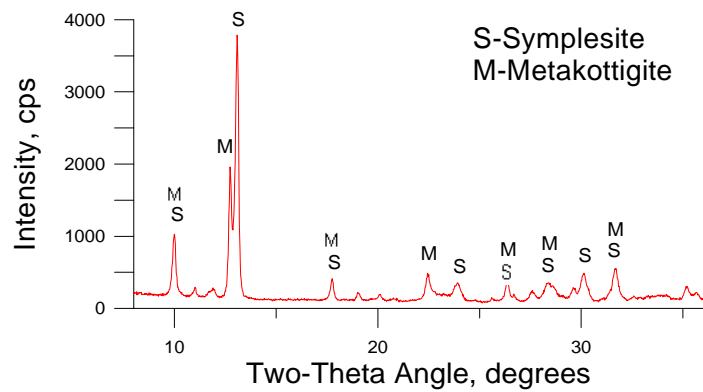
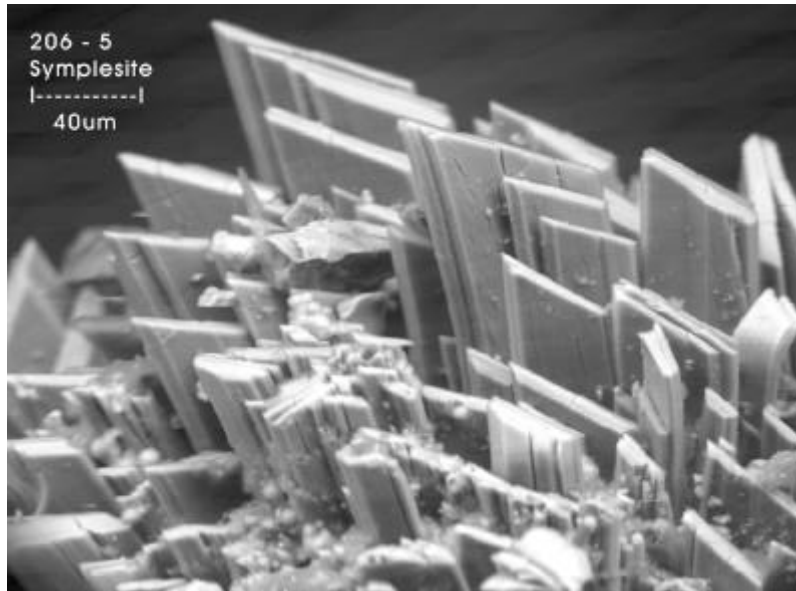


Figure 8. Scanning electron microscope BSE image and corresponding x-ray diffractogram of a coating on a slag fragment from splits of sample MW-206-5 (25 ft bgs). BSE image shows a cluster of symplectite crystals. Main peaks in XRD pattern are for symplectite ($\text{Fe}_3(\text{AsO}_4)_2 \cdot 8\text{H}_2\text{O}$) and metakottigite ($(\text{Fe,Zn})_3(\text{AsO}_4)_2 \cdot 8(\text{H}_2\text{O,OH})$). BSE image by Cannon Microprobe.

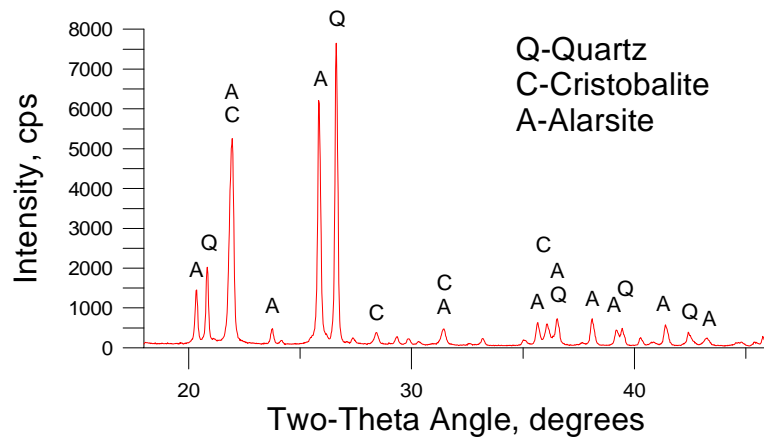
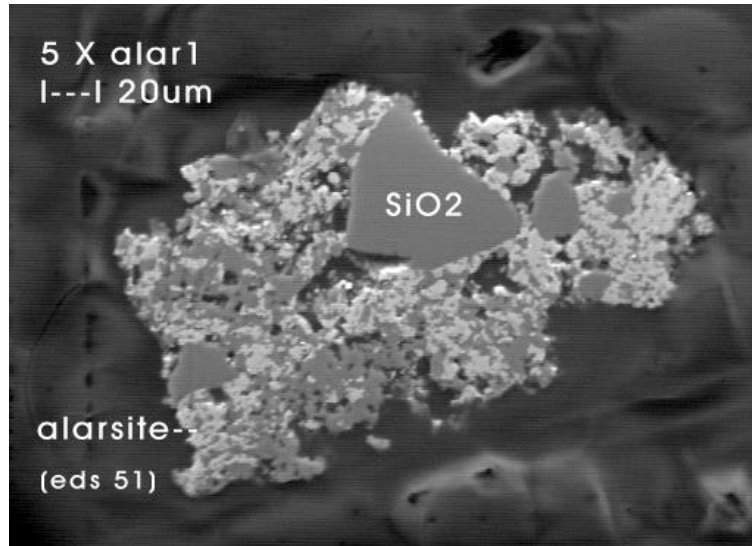


Figure 9. Scanning electron microscope BSE image and corresponding x-ray diffractogram of a fragment of silica sinter from splits of sample MW-206-5 (25 ft bgs). BSE image shows fine-grained alarsite filling the pore spaces between larger silica grains. Main peaks in XRD pattern are for quartz (SiO_2), cristobalite (also SiO_2), and alarsite (AlAsO_4). BSE image by Cannon Microprobe.

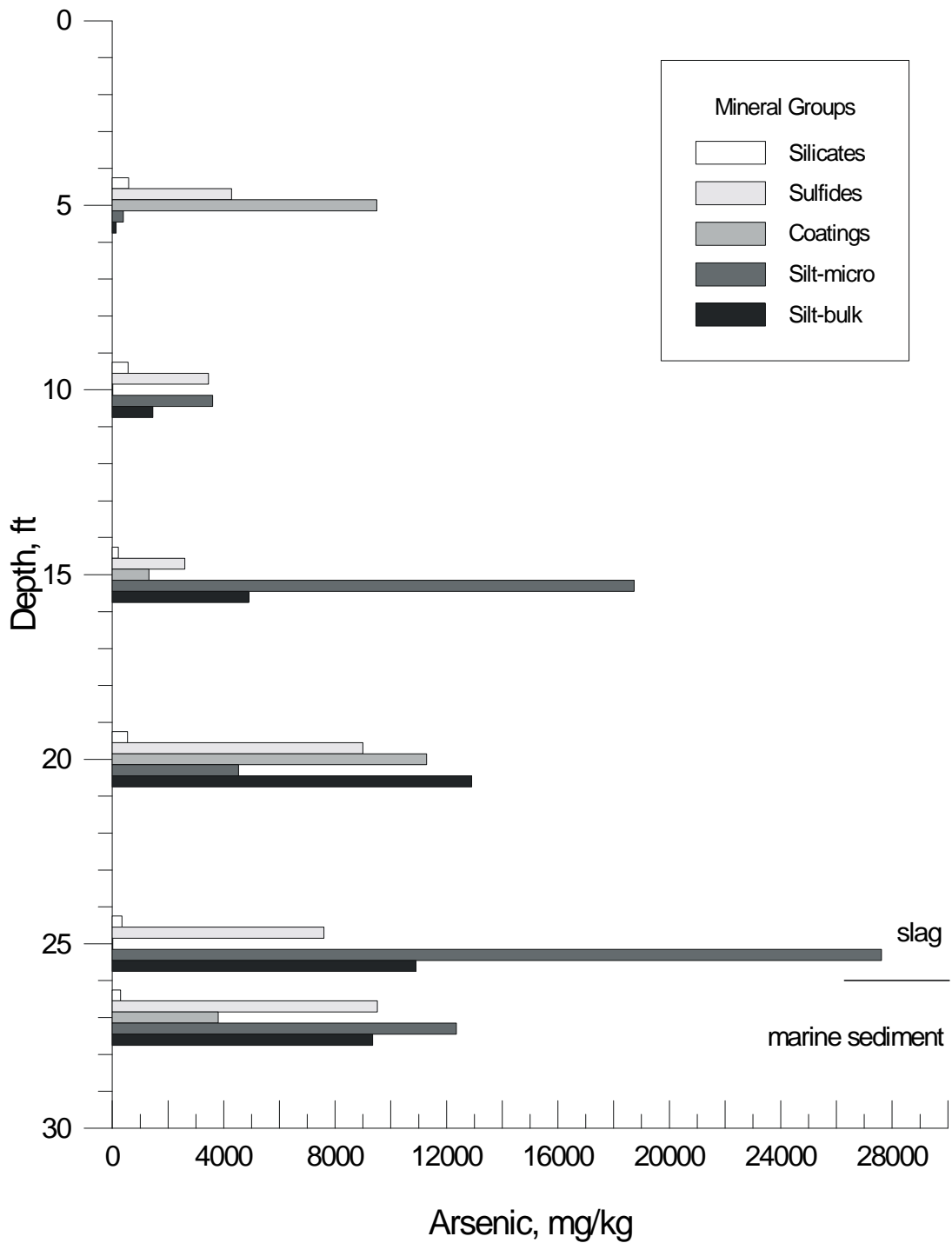


Figure 10. Comparison of arsenic concentration from bulk analysis and microanalysis of fines (silt fraction), and from microanalysis of three other groups of materials.

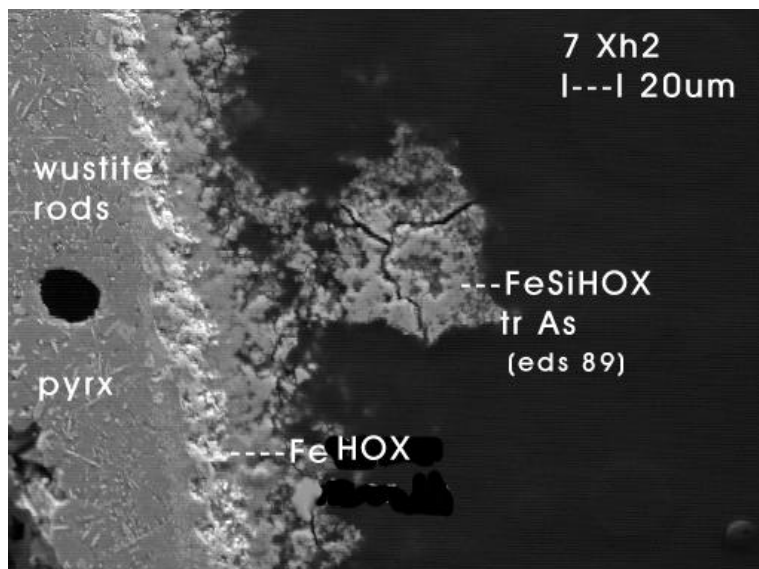
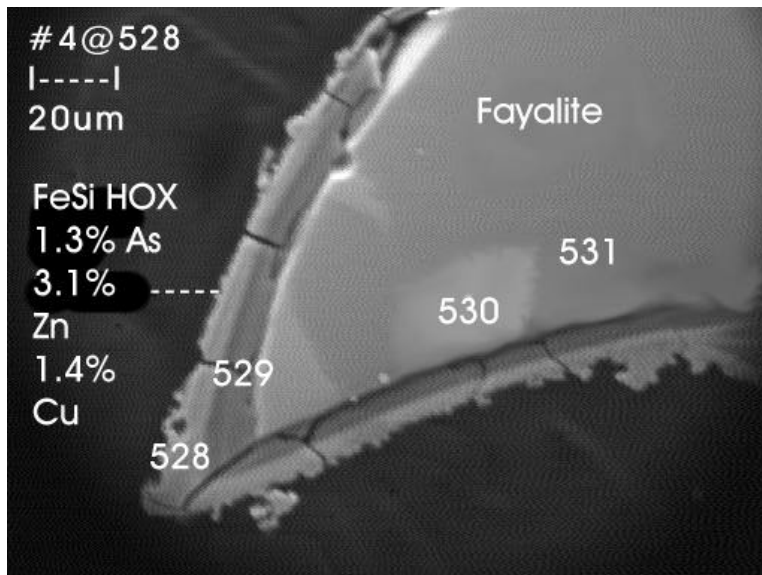


Figure 11. Scanning electron microscope BSE images of two contrasting substrates for coatings on slag fragments. The upper image from sample MW-206-4 shows a coating on a smooth underlying slag surface, indicating the coating probably precipitated from ground water. The lower image from sample MW-206-7 shows a coating on a heavily pitted slag surface, indicating the coating may have formed at least in part during alteration and recrystallization of the underlying slag. BSE images by Cannon Microprobe.

List of Tables

1. Field sample and corresponding laboratory sample numbers.
2. Field description for boring MW-206.
3. Summary list of secondary minerals.
4. Distribution of size separates, and corresponding arsenic concentrations.
5. List of arsenic concentrations from bulk analysis and microanalysis of borehole samples.

Table 1. Field sample and corresponding laboratory sample numbers.

<u>Hydrometrics field sample</u>	<u>EPA lab sample</u>	<u>Depth</u>	<u>Unit</u>
MW 206-1	97474450	5 ft	slag
MW 206-2	97474451	10 ft	slag
MW 206-3	97474452	15 ft	slag
MW 206-4	97474453	20 ft	slag
MW 206-5	97474454	25 ft	slag
MW 206-6	97474455	27 ft	marine sand and gravel
MW 206-7	97474456	5 depths*	slag

* Depths of slag fragments collected for MW-206-7 are 12.5, 13, 13.8, 15.5, and 19 ft.

Table 2. Field description for boring MW-206. Description is extracted from Hydrometrics, Inc., Test Log Field Form prepared by John Mefford, Hydrometrics.

Depth (ft)	Time PST	Description
November 18, 1997		
0-2		Sandy GRAVEL with cobbles and fines, light gray. [asphalt and slag, many quartz and lithic fragments] Slow drilling.
2-4		SAND, black. [slag]
5-6		SAND, black. [slag]
	1420	Sample MW-206-1
	1425	Sample MW-206-1D
8-9		Casing was driven easier.
November 19, 1997		
10-10.5		Gravelly SAND @ fines, black with metallic luster and light reddish-brown (~pumpkin orange) oxidation patina. [slag]
	0800	Sample MW-206-2
	0805	Sample MW-206-2D
12		Material same but cobbles more oxidized.
12.5		First indication of copper oxidized on slag cobbles, very light -green yellow.
12-12.5		Much water in bailed samples; water is orange-brown; indicates water table at 8-9 ft.
15-15.5		Gravelly SAND with fines, black with metallic luster similar to marcasite and reddish-brown patina on larger clasts. [slag] Slag is less oxidized than at 10 ft. Sample MW-206-3
16		Slow drilling; massive slag with little or no void spaces; bailer water is more grayish-brown rather than rust colored.
November 20, 1997		
19		Easier drilling; slag has many voids.
20-20.5		Gravelly SAND with silt, black, with reddish-brown patina on larger clasts. [slag]
	0855	Sample MW-206-4
	0900	Sample MW-206-4D
23		Slag is dark gray with metallic luster; looks similar to very fine-grained specular hematite. Massive slag with few voids.
25		Silty SAND, black with some reddish-brown patina and interspersed throughout is yellowish-white to light orange cinderstone (firebrick?). [slag and cinderstone]
	1205	Sample MW--206-5
26		Silty SAND with cinderstone and minor wood fragments.
27-28		Silty SAND, dark gray with dull white or pink shell fragments and white quartz clasts. [marine sand]
	1255	Sample MW-206-6
	1300	Sample MW-206-6D

Table 3. Summary list of secondary minerals in samples from borehole MW-206, as reported by XRD (Appendix B) and SEM/EPMA (Appendix C).

Sample MW-206-1 (slag - 5 ft)

SEM/EPMA

- FeSi hydroxide - sparse as coatings
- CuFe sulfate - alteration of copper iron sulfide prill

XRD

- none detected

Sample MW-206-2 (slag - 10 ft)

SEM/EPMA

- none detected

XRD

- none detected

Sample MW-206-3 (slag - 15 ft)

SEM/EPMA

- FeSi hydroxide - common in fines and somewhat common as coatings

XRD

- none detected

Sample MW-206-7 (slag fragments - 12-19 ft)

SEM/EPMA

- FeSi hydroxide - common as coatings
- CuFe sulfate and CuFeAs sulfate - as coatings
- CuZnPbFeAs hydroxide - alteration of sulfide
- Pb carbonate - single pore filling
- Ca sulfate - single pore filling

XRD

- Ferrihydrite ($\text{Fe}_5\text{O}_7\text{OH}\cdot 4\text{H}_2\text{O}$) - major amount in coatings
- Goethite (FeOOH) - trace amount in coatings
- Brochantite ($\text{Cu}_4\text{SO}_4(\text{OH})_6$) - minor amount in coating

Table 3 (continued). Summary list of secondary minerals in samples from borehole MW-206, as reported by XRD (Appendix B) and SEM/EPMA (Appendix C).

Sample MW-206-4 (slag - 20 ft)

SEM/EPMA

- FeSi hydroxide - common in fines and common as coatings
- FeCuPb sulfates, arsenates and hydroxides - minor intergrowth of alteration minerals with arsenides and sulfides
- Barite (BaSO_4)- single pore filling in Fe HOX
- Pb oxide or carbonate - single pore filling in FeSi HOX

XRD

- Ferrihydrite ($\text{Fe}_5\text{O}_7\text{OH}\cdot 4\text{H}_2\text{O}$) - minor amount in coating
- Goethite (FeOOH) - trace amount in coating and in fines

Sample MW-206-5 (slag - 25 ft)

SEM/EPMA

- FeSi hydroxide - somewhat common in fines and as coatings
- Alarsite (AlAsO_4) - abundant as inclusions in aluminous silica sinter
- Symplectite ($\text{Fe}_3(\text{AsO}_4)_2\cdot 8\text{H}_2\text{O}$) - as coating
- Variety of other arsenates (FePb arsenate?, Pb arsenate?, MgFeAl arsenate?, AlFe arsenate, FeSb arsenate?, FeSi arsenate?) - as inclusions in silica sinter and pore spaces of silicate slag

XRD

- Goethite (FeOOH) - trace amount in fines
- Alarsite (AlAsO_4) - major amount in silica sinter, minor amount in fines
- Symplectite ($\text{Fe}_3(\text{AsO}_4)_2\cdot 8\text{H}_2\text{O}$) - major amount in coating
- Parasymplesite ($\text{Fe}_3(\text{AsO}_4)_2\cdot 8\text{H}_2\text{O}$) - minor amount in coating and fines
- Metakottigite ($(\text{Fe,Zn})_3(\text{AsO}_4)_2\cdot 8(\text{H}_2\text{O,OH})$) - minor amount in coating

Sample MW-206-6 (marine sand and gravel - 27 ft)

SEM/EPMA

- FeSi hydroxide - somewhat common in fines and as coatings
- Alarsite (AlAsO_4) - abundant as inclusions in aluminous silica sinter
- Fe arsenate - single grain as pore filling
- FeCuZn arsenate? - single grain as pore filling
- FeCuSi sulfate? - as alteration of sulfide

XRD

- Goethite (FeOOH) - trace amount in fines
- Alarsite (AlAsO_4) - trace amount in fines

Table 4. Distribution of size separates for samples from borehole MW-206, and corresponding arsenic concentrations.

Sample	Unit	Depth ft	Size mm	Wt %	Arsenic mg/kg
MW-206-1	slag	5	>2	60	
			0.07-2	39	49.4
			<0.07	0.8	140
MW-206-2	slag	10	>20		
			2-20	54	
			0.07-2	45	105
			<0.07	0.8	1460
MW-206-3	slag	15	>2	59	
			0.07-2	40	161
			<0.07	1.3	4910
MW-206-4	slag	20	>20		
			2-20	54	
			0.07-2	44	168
			<0.07	2.2	12900
MW-206-5	slag	25	>20		
			2-20	15	
			0.07-2	83	57.8
			<0.07	2.4	10900
MW-206-6	marine	27	>20		
			2-20	57	
			0.07-2	42	1610
			<0.07	2.1	9360
MW-206-7	slag	12.5	>20		
		13	>20		
		13.8	>20		
		15.5	>20		
		19	>20		

Table 5. Arsenic concentrations from bulk analysis and microanalysis of borehole samples. Values for bulk analysis are from hydride generation/atomic absorption results for fine (silt) fraction of <0.07 mm (Appendix A). Values for microanalysis are the geometric means of WDS analyses grouped according to material type (Appendix C). For the averaging calculation, zero values in Appendix C are assigned a lower limiting value of 100 mg/kg. Missing values for coatings occur because the coatings results were lumped together with fines in Appendix C.

Sample _____	Depth ft bgs	Unit _____	Silt (A) mg/kg	Silt (C) mg/kg	Coating (C) mg/kg	Sulfide (C) mg/kg	Silicate (C) mg/kg
MW-206-1	5	slag	140	410	9500	4290	590
MW-206-2	10	slag	1460	3610	--	3450	570
MW-206-3	15	slag	4910	18700	1320	2600	220
MW-206-4	20	slag	12900	4540	11300	9010	550
MW-206-5	25	slag	10900	27600	--	7610	360
MW-206-6	27	marine	9360	12300	3800	9520	950